10600 *Macromolecules* **2010**, *43*, 10600–10611
DOI: 10.1021/ma101945f

Macromolecules
ARTICLE

Double Reaction-induced Microphase Separation in Epoxy Resin Containing Polystyrene-*block*-poly(ε-caprolactone)-*block*-poly-(*n*-butyl acrylate) ABC Triblock Copolymer

Wenchun Fan, Lei Wang, and Sixun Zheng*

Department of Polymer Science and Engineering and State Key Laboratory of Metal Matrix Composites, Shanghai Jiao Tong University, Shanghai 200240, P. R. China

Received August 23, 2010; Revised Manuscript Received November 9, 2010

ABSTRACT: Polystyrene-*block*-poly(ε-caprolactone)-*block*-poly(*n*-butyl acrylate) (PS-*b*-PCL-*b*-PBA) triblock copolymer was synthesized through the combination of atom transfer radical polymerization, copper-catalyzed Huisgen 1,3-dipolar cycloaddition and ring-opening polymerization. The PS-*b*-PCL-*b*-PBA ABC triblock copolymer was incorporated into epoxy to access the nanostructures in the thermoset. The microphase-separated morphology was investigated by means of atomic force microscopy (AFM), small-angle X-ray scattering (SAXS) and dynamic mechanical thermal analysis (DMTA). It was found that depending on the concentration of the triblock copolymer in the thermosets several kinds of nanodomains were formed and they were arranged in lamellar lattice. The formation of the nanostructures was ascribed to the tandem reaction-induced microphase separation of PBA and PS blocks in the thermosetting blends. The investigation of the model binary thermosetting blends showed that the phase separation of PBA occurred at the conversion much lower than that of PS. It is proposed that the PBA nanophases were formed prior to the PS nanophases in the thermosetting blends and the microdomains of PBA subchains could behave as the template for the demixing of PS blocks. The coupling of the two-stage reaction-induced microphase separation exerted a profound impact on the formation of nanostructures in the epoxy thermosets containing the ABC triblock copolymer. Thermal analysis shows that with the formation of the nanostructures in the thermosets a part of poly(ε-caprolactone) subchains were demixed from epoxy matrix; the fractions of demixed PCL blocks have been estimated according to the T_g-composition relation of the model binary blends of epoxy and PCL.

Introduction

Reaction-induced phase separation (RIPS) in multicomponent thermosets has been extensively investigated during the past few decades.[1,2] The driving forces for RIPS are attributed to two aspects: (i) the increased molecular weight owing to polymerization (viz. curing reaction), which gives rise to the decreased contribution of mixing entropy to the free energy of mixing; (ii) the alteration of the intercomponent interaction parameters (χ) with conversion of monomers. The latter may favor mixing or demixing, depending on whether χ decreases or increases with conversion. If the systems possess favorable intermolecular specific interactions (e.g., hydrogen bonding), the miscible blends of thermosets will be obtained.[3−9] If the χ was increased with conversion, the above collective changes may cause the systems to cross thermodynamic phase boundaries and result in a transition from an initial homogeneous state into a microphase-separated state. The final morphology of the thermosets is strongly dependent on the competitive kinetics involving curing reaction, phase separation and connectivity of phases. In the binary blends of thermosets containing one linear polymer, several types of phase-separated morphologies such as cocontinuous structures, uniform spherical domain and bimodal spherical domain structures have been accessed by modulating the competitive kinetics of curing process.[1,2] Some complicated morphologies can be formed in ternary blends of thermosets containing two linear polymers.[10−13]

Generally, RIPS takes place on the macroscopic scale since the modifiers are some homopolymers or random copolymers. If amphiphilic block copolymers are used as the modifiers, the phase separation might be confined to the micrometer scale, i.e., so-called reaction-induced microphase separation (RIMPS) occurs.[14] It has been demonstrated that nanophases can be formed in the thermosetting blends of epoxy with poly(ε-caprolactone)-*block*-polybutadiene-*block*-poly(ε-caprolactone) triblock copolymer via RIMPS mechanism.[15] It is of interest to note that some long-ranged nanostructures can be even obtained via this approach.[16] Recently, RIMPS has been recognized to be an efficient approach to obtain the thermosets with a variety of nanostructures.[17−25] It should be pointed out that Hillmyer et al.[26,27] have first proposed the strategy of self-assembly to access the nanostructures in thermosets. In this protocol, the precursors of thermosets act as the selective solvents of block copolymers and some self-organized nanostructures are formed in the mixtures before curing reaction. These preformed nanostructures are fixed through the subsequent curing reaction. In marked contrast to self-assembly approach, the formation of nanostructures in thermosets via RIMPS may be significantly affected by the competitive kinetics of curing reaction and microphase separation. During the past years, the self-assembly approach has been extensively investigated vis-à-vis RIMPS behavior in thermosets.[28−44] The modulation of nanostructures in thermosets via RIMPS remains largely unexplored.

In all the previous reports on the formation of nanostructures in thermosets by the use of block copolymers,[15−44] only a few reports have been concerned with the thermosets containing ABC triblock copolymers.[35,36,45] Rebizant et al.[35,36] have reported the formation of the ordered nanostructures in epoxy thermosets containing polystyrene-*block*-polybutadiene-*block*-poly(methyl methacrylate) ABC triblock copolymers (PS-*b*-PB-*b*-PMMA). In the

*To whom correspondence should be addressed. E-mail: szheng@sjtu.edu.cn. Telephone: 86-21-54743278. Fax: 86-21-54741297.

 Published on Web 12/01/2010

nanostructured thermosets PB blocks aggregates into spherical domains at the interface between the epoxy-rich matrix and spheres formed by the PS blocks. The swelling of the PMMA blocks by epoxy components induces a morphological transition from PB helices around PS cylinders, the morphology of the neat triblock copolymer, to PB spheres on PS spheres. It was found that the self-assembled PB nanophases are not affected by the reaction. The final structure is composed of undiluted PS and PB blocks, forming "spheres on spheres" morphology, most of the PMMA chains remaining embedded in the epoxy networks. More recently, Fan et al.[45] investigated the formation of nanostructures in epoxy containing polydimethylsiloxane-*block*-poly(ε-caprolactone)-*block*-polystyrene ABC triblock copolymer (PDMS-*b*-PCL-*b*-PS), in which the midblock (viz. PCL) is bound to two epoxy thermoset-immiscible blocks (i.e., PDMS and PS). Owing to the immiscibility of PDMS with epoxy precursors, the RIMPS of PS block in epoxy occurred in the presence of self-assembled PDMS nanophases and the preformed PDMS microphases have exerted a profound impact on the RIMPS of PS blocks. It should be pointed out that the presence of the self-organized nanophases prior to the curing reaction was involved with the formation of nanostructures in above two epoxy thermosets containing ABC triblock copolymers. To the best of our knowledge, there has been no precedent report on the formation of nanostructures in thermosets containing ABC triblock copolymer only via RIMPS.

In this contribution, we reported the formation of nanostructures in epoxy thermosets containing polystyrene-*block*-poly(ε-caprolactone)-*block*-poly(*n*-butyl acrylate) (PS-*b*-PCL-*b*-PBA) triblock copolymer. This ABC triblock copolymer contains two end blocks capable of microphase separation induced by reaction (viz. PS and PBA) in epoxy and one midblock miscible with epoxy. It is expected that double RIMPS occurs while the ABC triblock copolymer is incorporated into epoxy resin and the resulting microphase-separated morphology will be dependent on the competitive demixing kinetics between PS and PBA blocks from epoxy thermosets. In this work, the nanostructures of the thermosets were investigated by means of atomic force microscopy (AFM) and small-angle X-ray scattering (SAXS). Dynamic mechanical thermal analysis (DMTA) and differential scanning calorimetry (DSC) were employed to investigate the demixing behavior of PCL subchains with the occurrence of double reaction-induced microphase separation

Experimental Section

Materials. Diglycidyl ether of bisphenol A (DGEBA) with the epoxide equivalent weight of 185−210 was supplied by Shanghai Resin Co., China. 4,4′-Methylenebis(2-chloroaniline) (MOCA) was used as the curing agent, purchased from Shanghai Reagent Co., China. Styrene (St) and *n*-butyl acrylate (BA) are of analytically pure grade and were obtained from Shanghai Reagent Co., China. Prior to use, the inhibitor was removed by washing with aqueous NaOH solution (5 wt %) and deionized water for at least three times and dried by anhydrous Mg_2SO_4; the monomers were further distilled at reduced pressure. ε-Caprolactone (99%) was purchased from Fluka Co., Germany, and it was dried over calcium hydride (CaH_2) and distilled under decreased pressure. 2-Bromoisobutyryl bromide, methyl 2-bromopropionate (98%), propargyl alcohol (99%) and *N,N,N′, N″,N‴*-pentamethyldiethylenetriamine (PMDETA) were purchased from Aldrich Co. USA and used as received. Stannous octanoate [$Sn(Oct)_2$], copper(I) bromide (CuBr) and sodium azide (NaN_3) were obtained from Shanghai Reagent Co., China. Before use, Cu^IBr was purified according to the reported procedure.[46] Triethylamine was of analytically pure grade and was dried over CaH_2 and then was refluxed with *p*-toluenesulfonyl chloride, followed by distillation. All other solvents used in this work are obtained from commercial resources and were purified according to standard procedures.

Synthesis of Bromo-Terminated PS. Bromo-terminated polystyrene (PS−Br) was synthesized via atomic transfer radical polymerization (ATRP) and the complex of Cu^IBr with *N,N,N′, N″,N″*-pentamethyldiethylenetriamine (PMDETA) was used as the catalyst and methyl 2-bromopropionate as the initiator. Typically, methyl 2-bromopropionate (0.2839 g, 1.7 mmol), Cu^IBr (0.2492 g, 1.7 mmol), PMDETA (361 μL, 1.7 mmol), and St (0.1730 mol) were charged to a 50 mL round-bottom flask. The system was connected to the Schlenk line system, and three freeze−pump−thaw cycles were used to remove the trace of oxygen and moisture. The polymerization was carried out by immersing the flask into an oil bath at 110 °C for 2 h. The crude product was dissolved in tetrahydrofuran and passed through a neutral alumina column to remove the catalyst; the polymer solution was concentrated and dropped into excess cold methanol. The resulting product was dried *in vacuo* at 30 °C for 48 h. The polymer (10.5 g) was obtained by controlling the conversion of the monomer to be 56.7%. The ^1H NMR ($CDCl_3$, ppm): 6.3−7.3 (365.8H, C_6H_5 of styrene), 4.3−4.7 (0.52H, Br$CH$$CH_2$), 3.3−3.6 (3H, H_3COCO), 1.0−2.6 (247.0H, $CHCH_2$ methylene and methylene protons of styrene), 0.7−1.1 (3.72H, $H_3COCOCHCH_3CH$). The molecular weight of the product was measured to be M_n = 8200 with M_w/M_n = 1.10 by means of gel permeation chromatography (GPC) (see Figure 3).

Synthesis of Azido-Terminated PS. The azido-terminated polystyrene (PS−N_3) was synthesized by following the literature method.[47] Typically, 10.0 g (1.25 mmol) of bromo-terminated polystyrene (PS−Br) was dissolved in 80 mL of *N,N*-dimethylformamide and 0.1235 g (1.9 mmol) of sodium azide (NaN_3) was added. The reaction was performed with vigorous stirring at room temperature for 24 h. After that, the reacted mixture was precipitated into an excess cold methanol and the precipitates were collected and dried at 30 °C in a vacuum oven for 24 h and 9.48 g product was obtained with the yield of 95%. The ^1H NMR ($CDCl_3$, ppm): 6.30−7.32 (364.0H, C_6H_5), 3.86−4.06 (0.51H, N_3CHCH_2), 3.35−3.6 (3H, H_3COCO), 1.03−2.57 (234.3H, methine and methylene protons of PS main chain), 0.77−1.02 (3.66H, $H_3COCOCHCH_3CH$).

Synthesis of Hydroxyl-Terminated PS. To a 150 mL flask equipped with magnetic stirrer PS−N_3 (8.57 g, 1.071 mmol with respect of azido groups), Cu^IBr (51.4 mg, 0.350 mmol), PMDETA (74 μL, 0.350 mmol), and propargyl alcohol (0.12 g, 2.142 mmol) were charged. The system was connected a Schlenk line and three freeze−pump−thaw cycles were used to remove the trace of moisture and oxygen. The reaction was carried out at 25 °C for 24 h and then 20 mL of THF was added. The mixture was passed through a neutral alumina column to remove the catalyst. After that the solution was concentrated and dropped into an excess amount of cold methanol to obtain the precipitates with the yield of 95% after dried at 30 °C in a vacuum oven for 24 h. The ^1H NMR ($CDCl_3$, ppm): 6.3−7.3 (371.2H, C_6H_5 of styrene), 5.0−5.2 (0.57H, $C_6H_5CHN_3CHCCH_2OH$), 4.55−4.80 (1.11H, $C_6H_5CHN_3CHCCH_2OH$), 3.4−3.6 (3H, H_3COCO), 1.0−2.6 (235.1H, methine and methylene protons of PS main chain), 0.8−1.0 (3.36H, $H_3COCOCHCH_3CH$).

Synthesis of PS−*b*-PCL Diblock Copolymer. The above hydroxyl-terminated PS (PS−OH) (7.8700 g, 0.95 mmol with respect of hydroxyl groups) and ε-CL (10.5 g, 92.1 mmol) were charged to a 100 mL round-bottom flask equipped with a dry magnetic stirring bar and $Sn(Oct)_2$ (1/1000 by weight with respect to ε-CL) was added using a syringe. The flask was connected to a standard Schlenk line and three freeze−pump−thaw cycles were exerted to remove a trace of moisture and oxygen. The reactive system was then immersed in a thermostated oil bath at 110 °C for 24 h. The crude product was dissolved in 40 mL tetrahydrofuran and the solution was dropped into an excess amount of petroleum ether to afford the procipitates; this procedure was repeated three times to obtain white solids. The product was dried in a vacuum oven at room temperature and 17.36 g of polymer was obtained with the conversion of ε-CL to

be 91%. The molecular weight of PS-*b*-PCL−OH was determined by means of ^{1}H NMR spectroscopy and gel permeation chromatography (GPC). For ^{1}H NMR spectroscopy, the molecular weight of the PCL−OH was calculated according to the ratio of integration intensity of aliphatic methylene protons to protons of aromatic rings to be M_n = 8800. The GPC measurement gave the molecular weight of the diblock copolymer to be M_n = 18 400, M_w/M_n = 1.10.

Synthesis of PS-*b*-PCL-*b*-PBA Triblock Copolymer. The above hydroxyl-terminated polystyrene-*block*-poly(ε-caprolactone) diblock copolymer (PS-*b*-PCL−OH) was used to react with 2-bromoisobutyryl bromide in the presence of triethylamine to afford the 2-bromoisobutyryl-terminated PS-*b*-PCL [PS-*b*-PCL−OOCCBr$(CH_3)_2$], which was used to prepare polystyrene-*block*-poly(ε-caprolactone)-*block*-poly(*n*-butyl acrylate) (PS-*b*-PCL-*b*-PBA) triblock copolymer via atom transfer radical polymerization. Typically, PS-*b*-PCL−OOCCBr$(CH_3)_2$ (2.0110 g, 0.134 mmol), Cu(I)Br (19.30 mg, 0.134 mmol), PMDETA (28 μL, 0.134 mmol), *n*-BA (6.0128 g, 0.047 mol)and 4 mL of anhydrous xylene were charged to a 50 mL round-bottom flask. The system was connected to the Schlenk line system and three freeze−pump−thaw cycles were used to remove the trace of moisture and oxygen. The reactive system was immersed into an oil bath at 90 °C for 15 h. The crude product was dissolved in tetrahydrofuran and passed through a neutral alumina column to remove the catalyst; the polymer solution was dropped into an excess amount of cold methanol. The PS-*b*-PCL-*b*-PBA triblock copolymer was dried *in vacuo* at room temperature for 48 h. The polymer (4.18 g) was obtained by controlling the conversion of *n*-butyl acrylate monomer to be 36.2%. The molecular weight of the block copolymer was determined by means of gel permeation chromatography (GPC) to be M_n = 39 800 with M_w/M_n = 1.10 and thus the length of PBA subchain of the block copolymer is calculated to be M_n = 21 400.

Synthesis of Model PCL and PBA. The model poly(ε-caprolactone) (PCL) was synthesized via the ring-opening polymerization (ROP) of ε-CL with benzyl alcohol as the initiator, and $Sn(Oct)_2$ was used as the catalyst. Typically, benzyl alcohol (0.215 g, 2.0 mmol) and ε-CL (20.000 g, 175 mmol) were charged to a 50 mL round-bottom flask equipped with a dry magnetic stirring bar, and $Sn(Oct)_2$ (1/1000 by weight with respect to ε-CL) was added using a syringe. The flask was connected to a standard Schlenk line, and the reactive mixture was degassed via three freeze−pump−thaw cycles and then immersed in a thermostated oil bath at 120 °C for 36 h. The crude product was dissolved in tetrahydrofuran, and the solution was dropped into an excess amount of petroleum ether to afford the precipitates. This procedure was repeated three times to obtain white solids with the yield of 94%. The molecular weight of the PCL was estimated to be M_n = 9500 according to the ratio of integration intensity of aliphatic methylene protons to aromatic protons in its ^{1}H NMR spectrum.

The PBA with the molecular weight comparable to the length of PBA in the triblock copolymer was synthesized via atom transfer radical polymerization (ATRP), and methyl 2-bromopropionate was used as an initiator. BA (15.200 g, 118.4 mmol), Cu^IBr (0.0577 g, 0.4 mmol) and PMDETA (83 μL, 0.4 mmol) were charged to a 50 mL flask equipped with a magnetic stirrer, and 0.0668 g (0.4 mmol) methyl 2-bromopropionate was added with a syringe. The system was connected to the Schlenk line system, and three freeze−pump−thaw cycles were used to remove the trace of moisture and oxygen. The polymerization was carried out at 80 °C for 7 h and the conversion of BA was controlled within 58% and the molecular weight was determined to be M_n = 22 000.

Preparation of Binary Blends of Epoxy with PCL. The desired amount of the model PCL was dissolved in DGEBA and then the stoichiometric MOCA with respect of DGEBA was added with continuous stirring until the mixtures were homogeneous. The ternary mixture was poured into Teflon mold and cured at 150 °C for 4 h plus 180 °C for 2 h.

Preparation of Epoxy Thermosets Containing PS-*b*-PCL-*b*-PBA. The PS-*b*-PCL-*b*-PBA triblock copolymer was dissolved in DGEBA with continuous stirring and the curing agent MOCA was added to the mixtures with vigorous stirring until homogeneous solutions were obtained. The ternary mixture was poured into Teflon mold and cured at 150 °C for 4 h plus 180 °C for 2 h.

Measurement and Characterization. *Nuclear Magnetic Resonance Spectroscopy* (*NMR*). The samples were dissolved in deuterium chloroform and the NMR spectra were measured on a Varian Mercury Plus 400 MHz NMR spectrometer with tetramethylsilane (TMS) as the internal reference.

Gel Permeation Chromatography (*GPC*). Molecular weights and molecular weight distribution of polymers were determined on Waters 717 Plus autosampler gel permeation chromatography apparatus equipped with Waters RH columns and a Dawn Eos (Wyatt Technology) multiangle laser light scattering detector and the measurements were carried out at 25 °C with tetrahydrofuran (THF) as the eluent at the rate of 1.0 mL/min.

Phase Contrast Microscopy (*PCM*). A Leica DMLP polarized optical microscope equipped with a hot stage (Linkam TH960, Linkam Scientific Instruments, Ltd., U.K.) with a precision of ±0.1 °C was used for the determination of the onset of reaction-induced phase separation for the DGEBA-MOCA and PS (and/or PBA) mixtures. The THF solutions of the mixtures were cast onto cover glasses; the majority of the solvent was removed at room temperature and the residual solvent was further eliminated *in vacuo* at 50 °C for 2 h. The films of the blends were sandwiched between two cover glasses. The blend films were observed under the polarizing microscope in which the angle between the polarizer and analyzer was 45°.[48] The samples were rapidly heated up to 150 °C to record the evolution of micrograph at this temperature as a function of curing time. The micrographs were automatically recorded with an interval of 30 s with an SONY Hyper HAD digital color video camera until the morphology remains unchanged. The images were analyzed by using a public domain image processing and analysis program freely available from the US National Institutes of Health (Image J)[49] to obtain the plot of particle area fraction as a function of curing time.

Curing Behavior of Binary Blends of Epoxy and PS (*and/or PBA*). The equimolar mixture of DGEBA with MOCA and the model PS (and/or PBA) were dissolved in a smallest amount of tetrahydrofuran at room temperature. The majority of solvent was removed via rotary evaporation at room temperature and the mixture was further desiccated in a vacuum at 30 °C for 4 h to eliminate the residual solvent. The isothermal curing behavior was investigated by means of differential scanning calorimetry (DSC). First, the sample (about 5 mg) was rapidly heated up to 150 °C and the isothermal endothermic enthalpy was recorded as a function of time. The conversion of isothermal endothermic enthalpy [α(*t*)] as a function of curing time (*t*) was determined using the following equation:

$$\alpha(t) = \int_{t_0}^{t} \left(\frac{dH}{dt}\right) dt \Big/ \int_{t_0}^{\infty} \left(\frac{dH}{dt}\right) dt \qquad (1)$$

where t_0 is the time at which the sample reaches isothermal conditions, as indicated by a flat baseline after an initial spike in the thermal curves. The integral in the numerator is the enthalpy generated during the time $t - t_0$, and the integral in the denominator is the total enthalpy of curing.

Atomic Force Microscopy (*AFM*). The specimens of thermosets for AFM observation were trimmed using a microtome machine and the thickness of the specimens is about 70 nm. The morphological observation of the sample sections was conducted on a Nanoscope IIIa scanning probe microscope (Digital Instruments, Santa Barbara, CA) in tapping mode. A tip fabricated from silicon (125 μm in length with *ca.* 500 kHz resonant frequency) was used for scan, and the scan rate was 2.0 Hz.

Small-Angle X-ray Scattering (*SAXS*). The SAXS measurements were taken on a Bruker Nanostar system. Two-dimensional diffraction patterns were recorded using an image intensified CCD detector. The experiments were carried out at room

Scheme 1. Synthesis of PS-*b*-PCL-*b*-PBA Triblock Copolymer

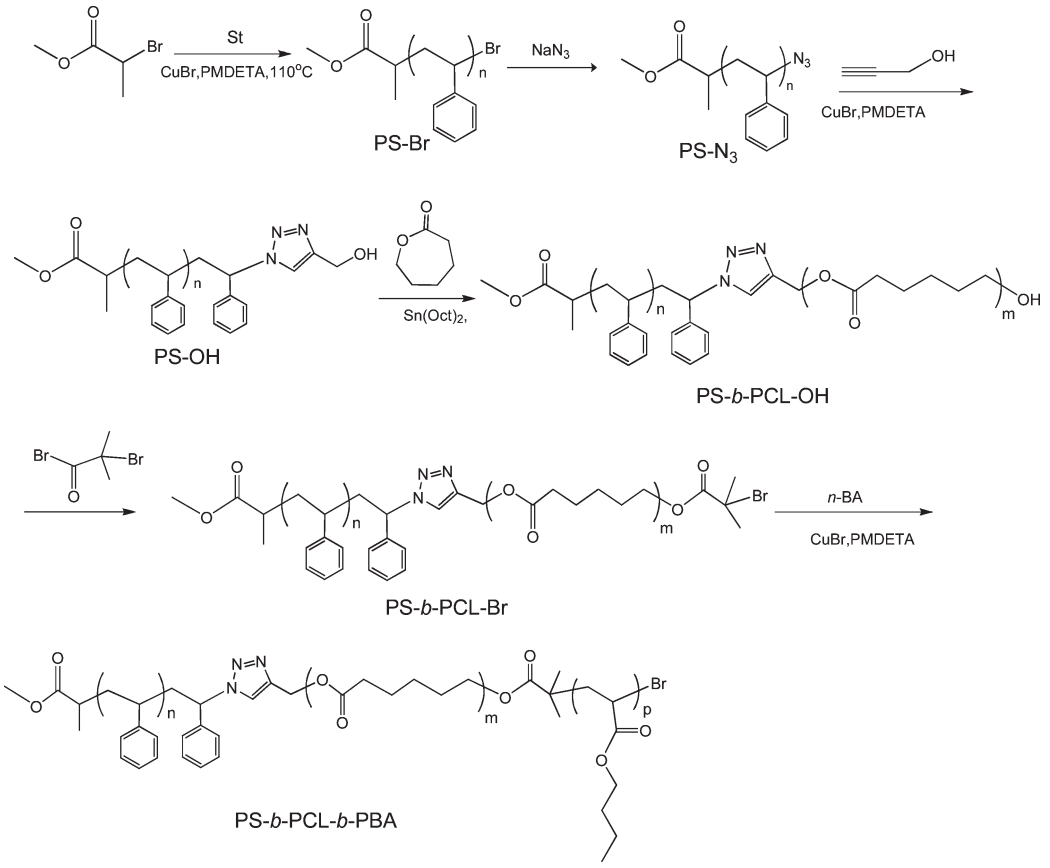

temperature (25 °C) using Cu Kα radiation (λ = 1.54 Å, wavelength) operating at 40 kV, 35 mA. The intensity profiles were output as the plot of scattering intensity (I) versus scattering vector, $q = (4\pi/\lambda)\sin(\theta/2)$ (θ = scattering angle). The variable temperature measurements were carried out on a small-angle X-ray scattering station (BL16B1) of Shanghai Synchrotron Radiation Facility (SSRF), Shanghai, China, in which the third generation of synchrotron radiation light source was employed. Two dimensional diffraction patterns were recorded using an image intensified CCD detector. The experiments were carried out with the radiation of X-ray with the wavelength of λ = 1.24 Å. A TH MS600 Linkam hotstage with the precision of 0.1 °C was mounted and used for the experiments of variable temperatures. The intensity profiles were output as the plot of scattering intensity (I) versus scattering vector, $q = (4\pi/\lambda)\sin(\theta/2)$ (θ = scattering angle).

Dynamic Mechanical Thermal Analysis (*DMTA*). The dynamic mechanical tests were carried out on a TA Instruments Q800 dynamic mechanical thermal analyzer (DMTA) equipped with a liquid nitrogen apparatus in a single cantilever mode. The frequency used is 1.0 Hz and the heating rate 3.0 °C/min. The specimen dimension was 25 × 5.0 × 2.0 mm^3. The experiments were carried out from −100 °C until the samples became too soft to be tested.

Differential Scanning Calorimetry (*DSC*). The calorimetric measurements were performed on a Perkin-Elmer Pyris 1 differential scanning calorimeter in a dry nitrogen atmosphere. An indium standard was used for temperature and enthalpy calibrations, respectively. The samples (about 8.0 mg in weight) were first heated to 180 °C and held at this temperature for 3 min to remove the thermal history, followed by quenching to −70 °C. A heating rate of 20 °C/min was used at all cases. Glass transition temperature (T_g) was taken as the midpoint of the heat capacity change. The melting points (T_m) were taken as the temperatures of the maximum of endothermic peak.

Results

Synthesis of PS-*b*-PCL-*b*-PBA Triblock Copolymer. The route of synthesis for polystyrene-*block*-poly(ε-caprolactone)-*block*- poly(*n*-butyl acrylate) (PS-*b*-PCL-*b*-PBA) triblock copolymer was summarized in Scheme 1. In the first step, the bromo-terminated polystyrene was synthesized through atomic transfer radical polymerization (ATRP) of styrene with methyl 2-bromopropionate as the initiator and the complex of CuBr with *N*,*N*,*N*′,*N*″,*N*″-pentamethyldiethylenetriamine as the catalyst. The bromo-terminated PS was used to react with excess sodium azide (NaN_3) to afford an azido-terminated PS. The copper-catalyzed Huisgen 1,3-dipolar cycloaddition[50−53] between the azido-terminated PS and propargyl alcohol was performed to obtain the hydroxyl-terminated PS. The hydroxyl-terminated PS was then used as the macromolecular initiator to obtain polystyrene-*block*-poly(ε-caprolactone) diblock copolymer (PS-*b*-PCL) via the ring-opening polymerization of ε-caprolactone (CL). The terminal hydroxyl groups of the PS-*b*-PCL diblock copolymer were employed to react with 2-bromoisobutyryl bromide to afford the macromolecular initiator for the polymerization of *n*-butyl acrylate via ATRP to obtain polystyrene-*block*-poly(ε-caprolactone)-*block*-poly(*n*-butyl acrylate) triblock copolymer (PS-*b*-PCL-*b*-PBA). The purpose to utilize the above route of synthesis is to obtain the ABC triblock copolymer with a miscible midblock (viz. PCL[54,55]) and two immiscible end blocks (i.e., PS, PBA) with respect of epoxy resin. Shown in Figure 1 are the ^{1}H NMR spectra of the bromo-, azido- and hydroxyl-terminated PS. In all the case, the signals at *ca.* 3.5 ppm are discernible and are assigned to the resonance of methyl protons from the initiator, methyl 2-bromopropionate. The bromo-terminated PS is characterized by the resonance of methine proton at 4.43 ppm. With the occurrence of substitution of bromide atom with azido group, the

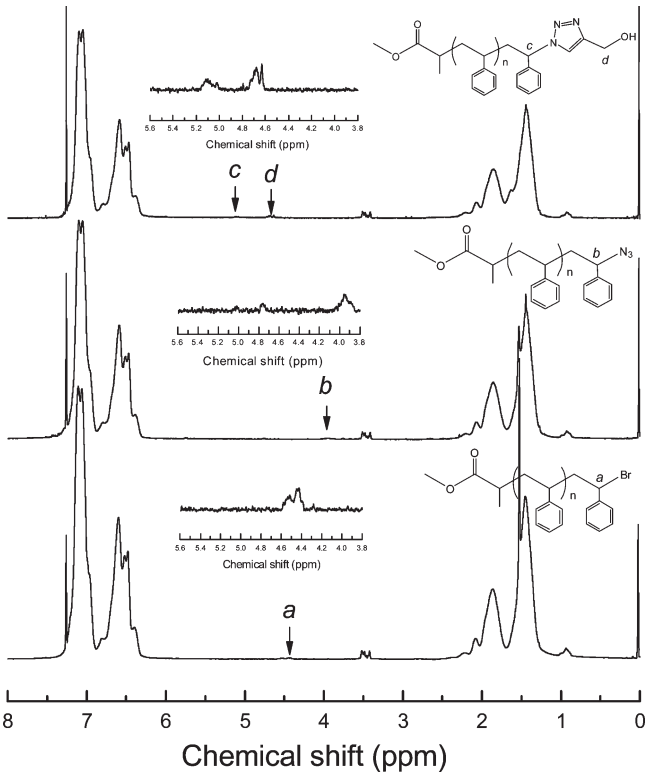

Figure 1. ^{1}H NMR spectra of Br-, azido- and hydroxyl-terminated PS.

resonance of the methine proton totally shifted to highfield at 3.96 ppm, suggesting that the reaction of substitution has been preformed to completion. It is seen that with the click reaction between the azido groups and propargyl alcohol, the resonance was observed to shift to 5.12 ppm. In the mean time, a new signal of resonance appeared at 4.65 ppm, which is assignable to the protons of methylene connected to both hydroxyl and triazole groups. The ^{1}H NMR spectroscopy indicates that the hydroxyl-terminated PS was successfully obtained, with which the subsequent ring-opening polymerization of ε-caprolactone (CL) and ATRP of *n*-butyl acrylate (BA) were carried out to afford the PS-*b*-PCL diblock and PS-*b*-PCL-*b*-PBA triblock copolymers. The ^{1}H NMR spectra of PS-*b*-PCL diblock and PS-*b*-PCL-*b*-PBA triblock copolymers are presented in Figure 2. For the PS-*b*-PCL diblock copolymer, the signals of resonance at 1.38 and 1.84 ppm are assignable to the protons of main-chain methylene and methine groups of PS block whereas the resonance in the range of 6.2−7.2 ppm is ascribed to the protons of aromatic rings of PS block. The PCL block is characterized by the signals of resonance at 1.38, 1.65, 2.3, and 4.1 ppm, assignable to the protons of methylene groups of PCL chains. It is noted that the resonance at 3.65 ppm is discernible and is ascribed to the protons of methylene at the terminal end of PCL chains. With the inclusion of PBA subchain, a new signal of resonance that is not overlapped with the other resonance of protons were detected at 0.93 ppm, which is ascribed to methyl groups. The ^{1}H NMR spectroscopy indicates that the resulting copolymer combined the structural features from PS, PCL, and PBA. The above bromo-terminated PS, PS-*b*-PCL diblock and PS-*b*-PCL-*b*-PBA triblock copolymers were subjected to gel permeation chromatography (GPC) and the curves of GPC are shown in Figure 3. It is seen that in all the cases, each GPC curve displayed a unimodal peak with the polydispersity of molecular weight to be *ca.* 1.10, suggesting that the polymerizations (viz. ROP and ATRP) were in living fashions. For the bromo-terminated PS, the GPC gave the molecular weight of M_n = 8200 with

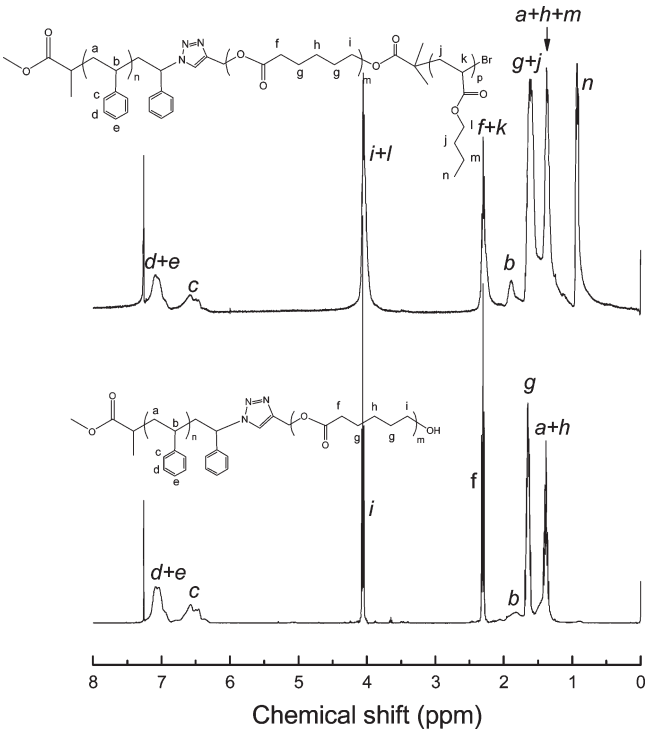

Figure 2. ^{1}H NMR spectra of PS-*b*-PCL diblock and PS-*b*-PCL-*b*-PBA triblock copolymer.

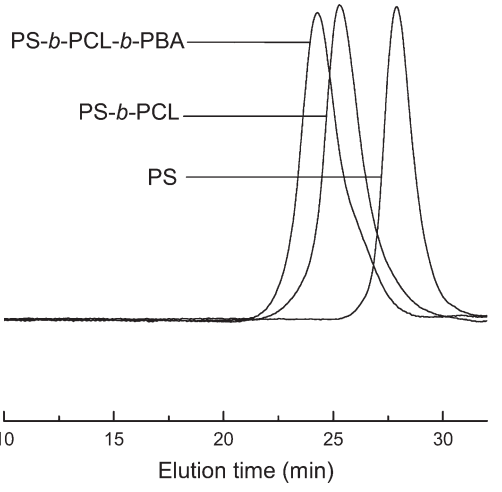

Figure 3. GPC curves of PS−Br, PS-*b*-PCL and PS-*b*-PCL-*b*-PBA.

M_w/M_n = 1.10. For the PS-*b*-PCL diblock copolymer, the molecular weight was measured to be M_n = 18 400 with M_w/M_n = 1.10. The result of GPC shows that the resulting ABC triblock copolymer possessed the molecular weight of M_n = 39 800 with M_w/M_n = 1.10. The results of ^{1}H NMR spectroscopy and GPC indicates that the PS-*b*-PCL-*b*-PBA triblock copolymer was successfully obtained.

Microphase Separation in Epoxy Thermosets Containing PS-*b*-PCL-*b*-PBA. The PS-*b*-PCL-*b*-PBA triblock copolymer was incorporated into epoxy to access the nanostructures in the thermosets. Before curing, all the mixtures composed of the precursors of epoxy (viz. DGEBA + MOCA) and the triblock copolymer were homogeneous and transparent. The mixtures were cured at elevated temperatures to obtain the thermosets with the content of PS-*b*-PCL-*b*-PBA triblock copolymer up to 40 wt %. It was seen that all the epoxy thermosets containing PS-*b*-PCL-*b*-PBA triblock

copolymer were homogeneous and transparent. The clarity suggests that no macroscopic phase separation occurred with the curing reaction. Nonetheless, the microphase separation cannot be excluded since the ABC triblock copolymer contains two blocks (viz. PS and PBA) which are immiscible with epoxy thermosets. In order to investigate the morphology of the thermosets, the thermosets were ultrathin trimmed and the sections were subjected to the observation by means of atomic force microscopy (AFM). The AFM micrographs of the thermosets were presented in Figure 4. The left and right images are the topography and phase contrast images, respectively. It is seen that in all the cases the epoxy thermosets containing PS-*b*-PCL-*b*-PBA triblock copolymer displayed the microphase-separated morphology. In views of the weight fraction of the components in the thermosets the dispersed microdomains are ascribed to the immiscible blocks (viz. PS and/or PBA). For the thermoset containing 10 wt % PS-*b*-PCL-*b*-PBA triblock copolymer, the irregular nanodomains with the size of 10−20 nm were dispersed in the continuous epoxy matrix. Some of them were spherical whereas others were worm-like (Figure 4A). With increasing the content of the triblock copolymer, the morphology of the thermosets changed significantly. For the thermoset containing 20 wt % PS-*b*-PCL-*b*-PBA triblock copolymer, a combined morphology was displayed. It is seen that there were some vesicle-like objects at the size of 20−40 nm besides some spherical nanodomains dispersed in the continuous epoxy matrix (Figure 4B). When the content of PS-*b*-PCL-*b*-PBA triblock copolymer is 30 wt % the lamellar nanostructures appeared. In some regions, the orientation direction of the cylinder axes is approximately parallel to the surface of fractured ends (Figure 4C). It is of interest to see that some lamellar nanophases were organized into "big co-centered cycles". When the concentration of PS-*b*-PCL-*b*-PBA triblock copolymer is 40 wt % the nanophases were organized into a well-defined lamellar morphology (see Figure 4D). It is proposed that in these lamellar nanostructures each layer was composed of both PS and PBA nanodomains, i.e., PS (and/or PBA) block did not form separate layer. The microphase-separated morphology was further investigated by means of small-angle X-ray scattering (SAXS).

Shown in Figure 5 are the SAXS profiles of the epoxy thermosets containing 10, 20, 30, and 40 wt % PS-*b*-PCL-*b*-PBA triblock copolymer. It is seen that the scattering peaks were observed in all the cases, indicating that the thermosets are microphase-separated. For the thermoset containing 10 wt % PS-*b*-PCL-*b*-PBA triblock copolymer a single scattering peak was detected at $q = 0.13\ \mathrm{nm}^{-1}$. The appearance of the single scattering maximum suggests that the thermoset was microphase-separated but the nanostructure was not ordered. Nonetheless, the nanophases gradually became long-ranged ordered. It is seen that while the content of PS-*b*-PCL-*b*-PBA triblock copolymer is 20 wt % or higher the multiple scattering maxima were detected. The degree of ordering was significantly enhanced with the increasing the content of PS-*b*-PCL-*b*-PBA triblock copolymer. According to the position of each first-order scattering peak, the Bragg's spacing d_m values were obtained to be 49.8, 49.7, 44.9, and 37.5 nm for the thermosets containing 10, 20, 30, and 40 wt % of PS-*b*-PCL-*b*-PBA triblock copolymer, respectively. It is noted that the positions of the first-order scattering peaks slightly shifted to the higher q values with increasing the content of PS-*b*-PCL-*b*-PBA triblock copolymer, suggesting that the average distance between neighboring domains decreased with increasing the content of the triblock copolymer. For the thermosets containing 20 wt % (and/or higher) PS-*b*-PCL-*b*-PBA triblock copolymer, the scattering peaks at the q values of 1, $4^{0.5}$, and $9^{0.5}$ relative to the first-order scattering peak positions (q_m) are discernible, implying that the nanodomains could be arranged into lamellar lattice. This result is in a good agreement with those obtained by means of AFM.

Discussion

Double Reaction-Induced Microphase Separation. With respect of the epoxy thermoset based on a stoichiometric mixture of diglycidyl ether of bisphenol A and 4,4′-methylenebis(2-chloroaniline), the PS-*b*-PCL-*b*-PBA triblock copolymer is composed of a miscible midblock (i.e., PCL) and two immiscible end blocks (viz. PS and PBA). Before curing, the mixtures with the compositions investigated were homogeneous and transparent at room and curing temperature (viz. 150 °C). The homogeneity was examined by means of small-angle X-ray scattering. Representatively shown in Figure 6 are the SAXS profiles of the mixture containing 40 wt % PS-*b*-PCL-*b*-PBA triblock copolymer at room temperature and 150 °C. The featureless scattering profiles indicate that the mixtures were miscible at the segmental level and no microphase separation was detected before curing reaction. After curing, the reaction-induced microphase separation involving PS and PBA blocks occurred, which was readily confirmed by means of dynamic mechanical thermal analysis (DMTA). The DMTA curves of the control epoxy and nanostructured thermosets containing PS-*b*-PCL-*b*-PBA ABC copolymer are shown in Figure 7. The control epoxy exhibited a well-defined relaxation peak (i.e., α transition) centered at *ca.* 160 °C, which is responsible for the glass−rubber transition of the cross-linked polymer. Apart from the α transition, the MOCA-cured epoxy exhibited a secondary transition (viz. β-relaxation) at the lower temperature (∼−60 °C) and at *ca.* 75 °C. The former is attributed predominantly to the motion of hydroxyl ether structural units [−CH_2−CH(OH)−CH_2−O-] whereas the latter to that of diphenyl groups in amine-cross-linked epoxy.[56−58] It is seen that upon adding PS-*b*-PCL-*b*-PBA into the thermosets, the α transition shifted to the lower temperatures but the β relaxation became indiscernible. The T_g's of the epoxy matrix decreased with increasing the content of PS-*b*-PCL-*b*-PBA triblock copolymer. The decreased T_g's are ascribed to the plasticization of PCL subchains on the epoxy matrix. In addition, there appeared two new transitions at −24 and +62 °C, respectively; the intensity of which increased with increasing the concentration of PS-*b*-PCL-*b*-PBA. The two peaks are assignable to the glass transitions of PBA and PS microdomains in the nanostructured thermosets, respectively. The appearance of these three glass transitions in the DMTA curves of the thermosets containing PS-*b*-PCL-*b*-PBA triblock copolymer demonstrates that the nanostructured morphologies in the epoxy thermosets were composed of three kinds of microphases, i.e., PS, PBA microdomains and epoxy matrix. The results of SAXS and DMTA indicate that the double reaction-induced microphase separation indeed occurred in the thermosetting blends containing PS-*b*-PCL-*b*-PBA triblock copolymer.

Effect of Double Reaction-Induced Microphase Separation on Nanostructures. In the previous work, it has been demonstrated that the reaction-induced microphase separation can occur in the thermosetting blends of epoxy with PCL-*b*-PS and/or PCL-*b*-PBA diblock copolymers.[20,21] In these thermosetting blends of PCL block remained miscible with the MOCA-cured epoxy thermosets via the formation of intermolecular hydrogen bonding interactions between the carbonyl groups of PCL and the hydroxyl groups of epoxy thermoset. In the present thermosetting blends of epoxy with

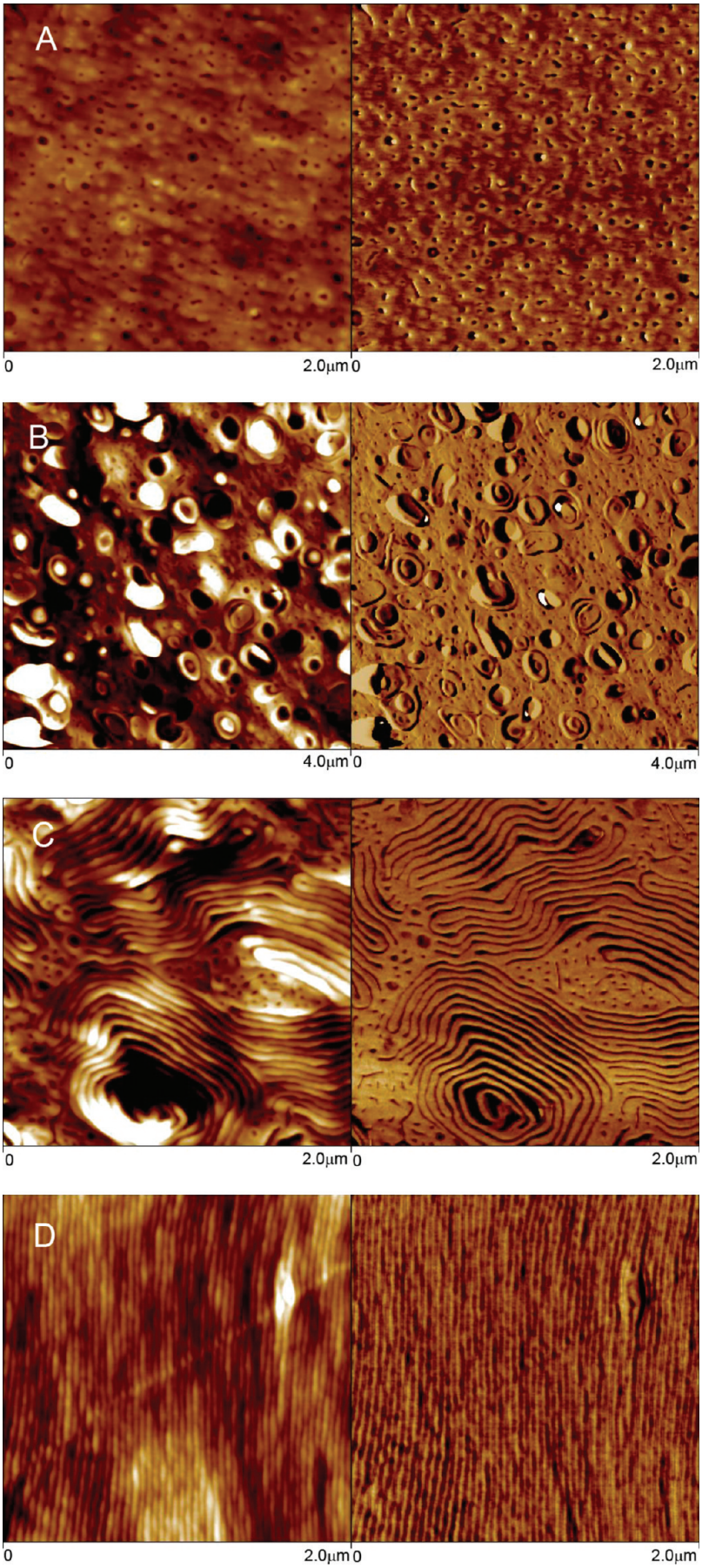

Figure 4. The AFM images of the epoxy thermosets containing (a) 10, (b) 20, (c) 30, and (d) 40 wt % of PS-*b*-PCL-*b*-PBA block copolymer. Left: topography; right: phase contrast images;.

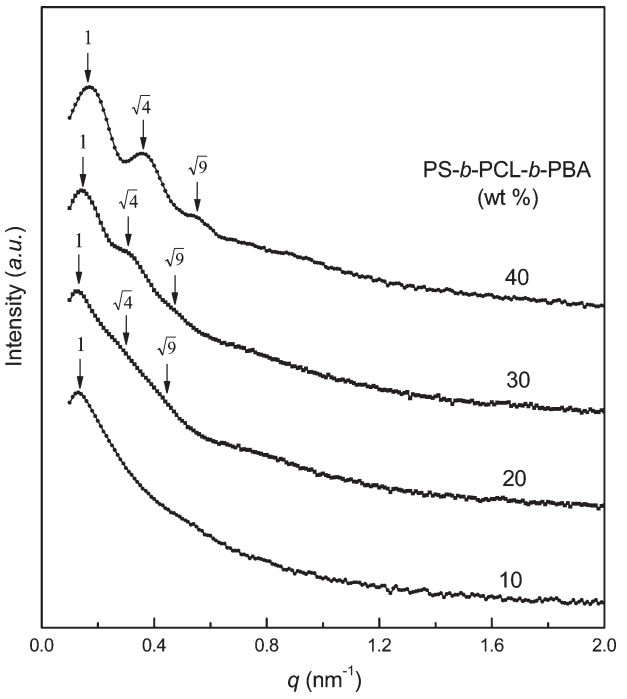

Figure 5. SAXS profiles of epoxy thermosets containing PS-*b*-PCL-*b*-PBA triblock copolymer. Each profile has been shifted vertically for clarity.

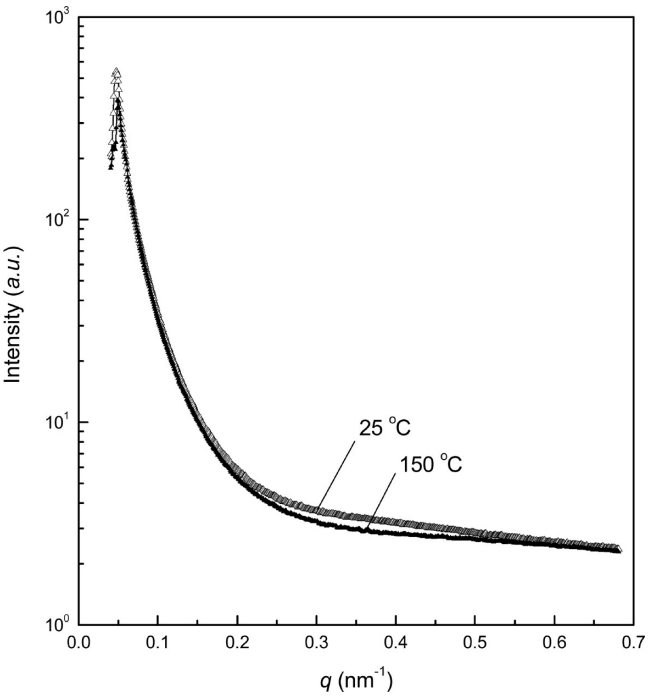

Figure 6. SAXS profiles of the mixture of precursors of epoxy (viz. equimolar mixture of DGEBA and MOCA) and 40 wt % PS-*b*-PCL-*b*-PBA triblock copolymer;.

PS-*b*-PCL-*b*-PBA triblock copolymer, the double reaction-induced microphase separation occurred, which is involved with PS and PBA blocks whereas the midblock (i.e., PCL) remains miscible with epoxy after and before curing reaction. However, the formation of the nanostructures in epoxy thermosets containing the ABC triblock copolymer is much complicated than those only containing PS-*b*-PCL or PCL-*b*-PBA diblock copolymer. The complication results from the competitive reaction-induced microphase separation of PS and PBA blocks in the thermoset. It is plausible to propose that the demixing of these two blocks (viz. PBA and PS) would occur at different conversion of epoxy precursors, i.e., the microdomains of one block are formed prior to those of another block. Owing to the connectivity of copolymer blocks, the early formed microdomains could act as the template of the reaction-induced microphase separation of another block and confine the microphase separation around the preformed nanophases. When the content of ABC triblock copolymer is relatively low, the early formed microdomain could possess spherical shape, which could be surrounded by the circles of another nanophase. With increasing the concentration of ABC triblock copolymer, the early formed microdomains could become interconnected (worm-like). The interconnected (or worm-like) microdomains will template the RIMPS of secondary subchains into the lamellar structures and thus the large-scaled lamellar nanostructures were obtained.

For the present epoxy thermosetting blends containing PS-*b*-PCL-*b*-PBA ABC triblock copolymer, it is of interest to know the relative rates of microphase separation of these two immiscible blocks (viz. PS and PBA) in epoxy. Toward this end, we examined the kinetics of reaction-induced phase separation in the blends of epoxy with the model PS and/or PBA homopolymers which possessed the identical molecular weights with the lengths of the corresponding subchains in the PS-*b*-PCL-*b*-PBA triblock copolymer. The mixtures containing the precursors of epoxy and the model PBA (and/or PS) were subjected to phase-contrast microscopy at the curing temperature (i.e., 150 °C) and the onset of reaction-induced phase separation was judged on the basis of the change of transmittance as a function of curing time. The phase-separated morphology was analyzed by using a domain image analysis program[49] to obtain the fraction of the demixed domains. Representatively shown in Figure 8 are the plots of domain area fraction as functions of curing time for the epoxy blend of containing 12.1 wt % PS and/or 26.4 wt % PBA, which corresponds to the contents of PS and/or PBA in the nanostructured thermoset containing 40 wt % PS-*b*-PCL-*b*-PBA triblock copolymer. It is seen that the domain area of the blends remained invariant for a long time after the curing reaction was initiated. After the induction period was elapsed the phase separation induced by reaction occurred as indicated by the abrupt increase in domain area fraction. For the blend of epoxy with the model PBA of 26.4 wt % the onset time of the phase separation was determined to be *ca.* 29 min, which corresponds to the conversion of epoxy monomers to be 16.8%. For the blend of epoxy with the model PS of 12.1 wt % the onset time of phase separation was *ca.* 34 min. In terms of the analysis of isothermal curing kinetics by means of DSC, the curing reaction within this time corresponded to the conversion of epoxy monomers to be 37.3%. It is noted that the phase separation of the model PBA was almost completed at *ca.* $T_{end} = \sim 33$ min, at which the demixing of PS has not been started. Therefore, it is judged that with the identical conditions the reaction-induced phase separation of PBA would be much in advance to that of PS. Therefore, the PBA subchains were first separated out to form spherical or interconnected nanophases depending on the concentration of the triblock copolymer with the curing reaction in the epoxy thermosets containing PS-*b*-PCL-*b*-PBA triblock copolymer. Owing to the connectivity of PCL midblock with PBA and PS end blocks, the preformed PBA nanophases could act as the templates of the reaction-induced microphase separation of PS subchains and confine the microphase separation of the PS subchains around the PBA nanophases. When the content of PS-*b*-PCL-*b*-PBA triblock copolymer is relatively low, the PBA subchains could be demixed into separate

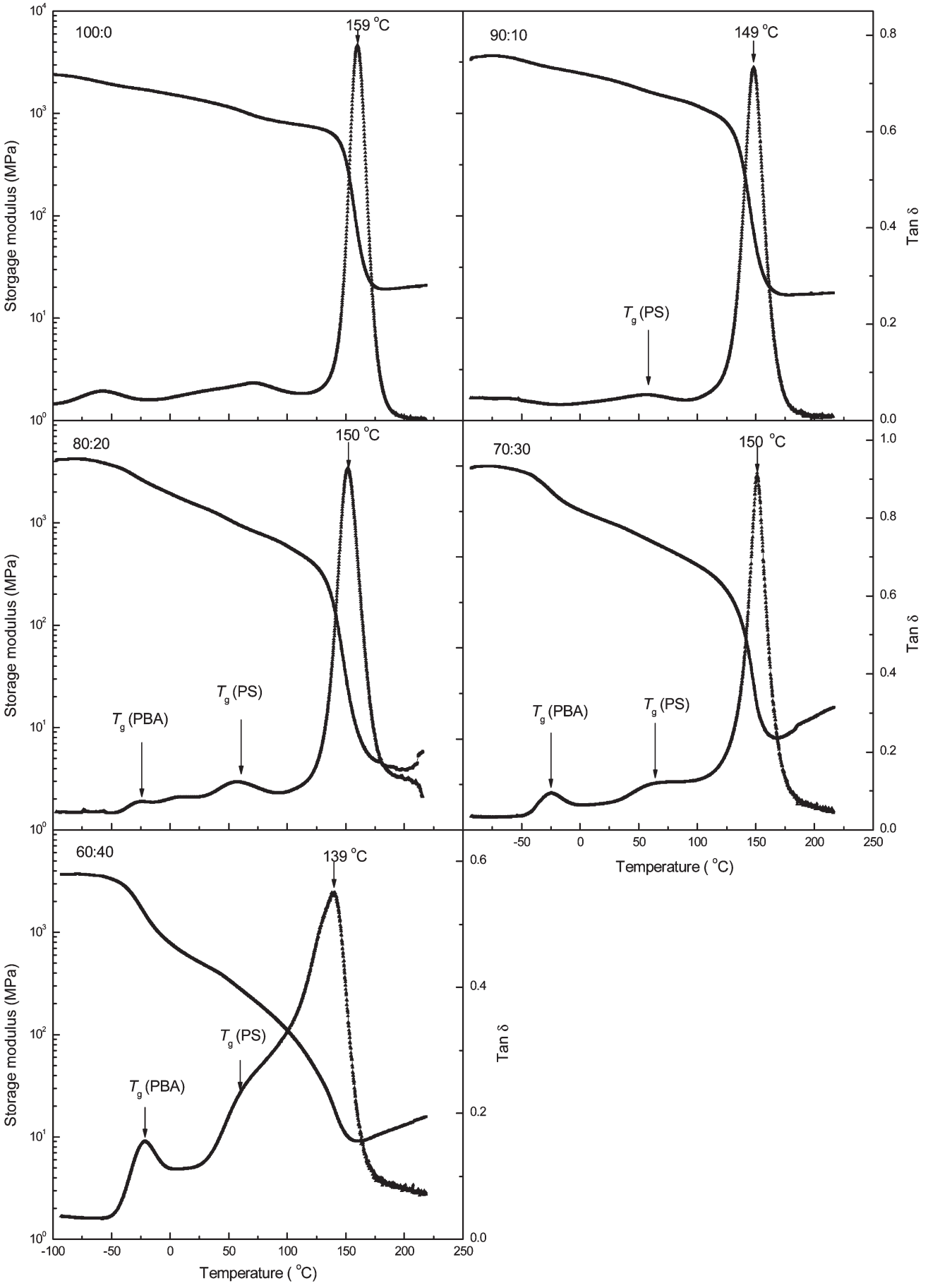

Figure 7. DMTA curves of control epoxy and the nanostructured thermosets containing PS-*b*-PCL-*b*-PBA triblock copolymer.

spherical particles, which were surrounded by the circles of PS nanophases (see Figures 4A and 4B). With increasing the concentration of PS-*b*-PCL-*b*-PBA, the predemixed PBA nanophases became interconnected nanoobjects (See Figures 4C and 4D). The interconnected (or worm-like) PBA nanophases will template the RIMPS of PS subchains into the lamellar structures and thus the large-scaled lamellar nanostructures were obtained for the thermosets containing 30 and 40 wt % PS-*b*-PCL-*b*-PBA triblock copolymer. The formation of nanostructures in the epoxy thermosets containing PS-*b*-PCL-*b*-PBA triblock copolymer can be depicted in Scheme 2. It should be pointed out that observation that the demixing for PBA block was earlier than that of PS block could result from the intermolecular interaction parameter (χ) in the epoxy and PBA blends higher than that in the epoxy and PS blends, which can be estimated according to solubility parameters.[59]

Demixing of PCL Block from Matrix. It has been reported that with the occurrence of curing reaction miscible blocks could be demixed from epoxy matrix to some extent in the nanostructured thermosets containing the amphiphilic diblock copolymer.[26,27] In the nanostructured thermosets via self-assembly mechanism, the demixing behavior has been interpreted as a transition from equilibrium morphology to a chemically pinned metastable state as the cross-linking reaction progresses through the gel point.[26,27] More recently, the demixing behavior of miscible blocks was also found in the nanostructured epoxy thermosets via reaction-induced microphase separation mechanism.[21,23] It is proposed that before curing reaction, all the subchains of block copolymers are miscible with the precursors of epoxy owing to the non-negligible contribution of mixing entropy to mixing free energy. With the occurrence of curing reaction the subchains immiscible with epoxy are separated out to form the nanophases due to the decrease in mixing entropy (ΔS). Nonetheless, there are the regions of depletion at the vicinity of the interface for the nanophases due to the restriction of networks and thus some miscible subchains become unmixed with the matrix.

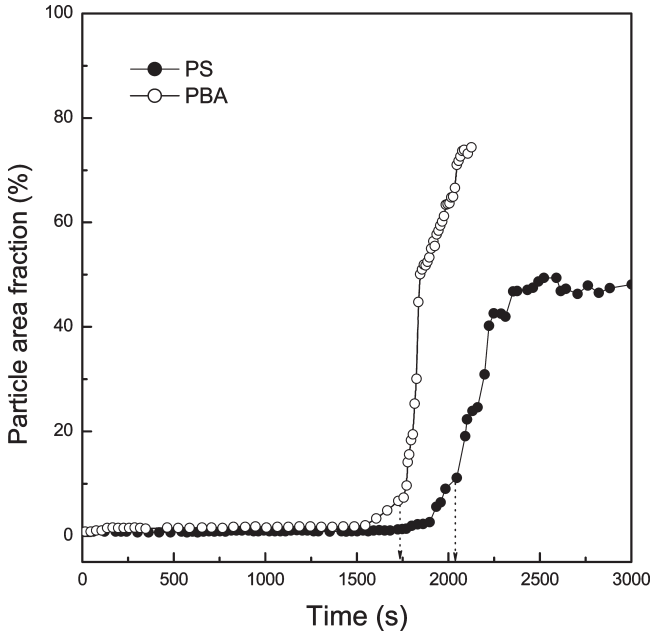

Figure 8. Plots of domain area fraction of the model PS of 12.1 wt % and the model PBA of 26.4 wt % as functions of curing time at 150 °C.

In the present case, the miscible midblock was connected to two immiscible end block (viz. PBA and PS). It is of interest to examine the demixing degree of the PCL chains with epoxy matrix. Toward this end, the nanostructured thermosets containing PBA-*b*-PCL-*b*-PS triblock copolymer were subjected to differential scanning calorimetry (DSC) and the DSC curves of the control epoxy, PBA-*b*-PCL-*b*-PS and their thermosetting blends are shown in Figure 9. The glass transition temperature (T_g) of the control epoxy is about 151 °C. In the DSC curve of PS-*b*-PCL-*b*-PBA triblock copolymer, a sharp melting transition at *ca.* 51 °C and two glass transitions are displayed at *ca.* −60 and 90 °C, respectively. The melting transition is ascribed to the crystalline PCL block whereas the glass transitions are responsible for the PBA and PS blocks, respectively. The fact that the melting transition of PCL block appeared prior to the glass transition of PS block indicates that the triblock copolymer is microphase-separated. It is noted that all the thermosets investigated did not exhibit the melting transition of PCL block, suggesting that the PCL blocks were trapped in the epoxy networks and became no longer crystalline, i.e., the PCL block are miscible with the epoxy networks. The miscibility was further evidenced by the depression in glass transition temperatures (T_g's) of the epoxy-rich phases as shown in Figure 9. The T_g value of the epoxy matrix can be employed to evaluate the mixing status of the PCL block with epoxy matrix.

In miscible polymer blends, the dependence of T_g on composition can be accounted for with several theoretical

Scheme 2. Double Reaction-Induced Microphase Separation in Thermosetting Blends of Epoxy with PS-*b*-PCL-*b*-PBA Triblock Copolymer

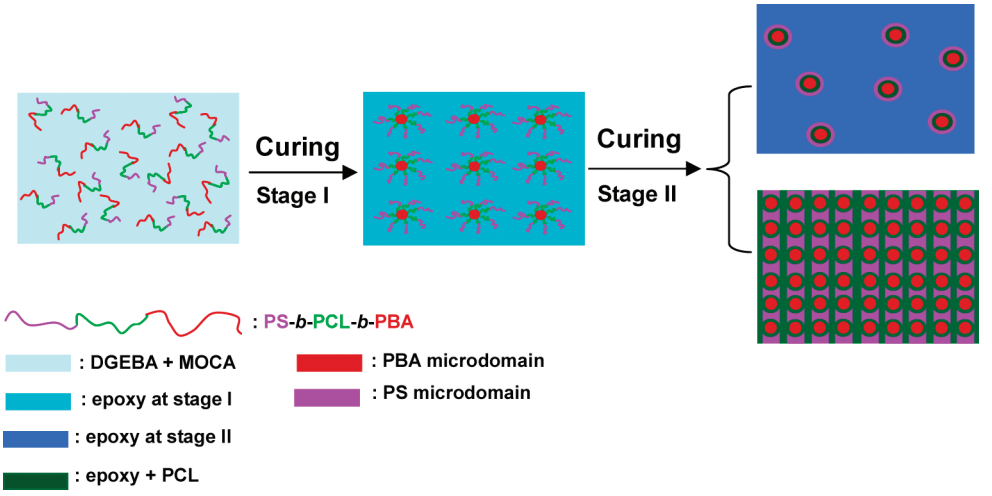

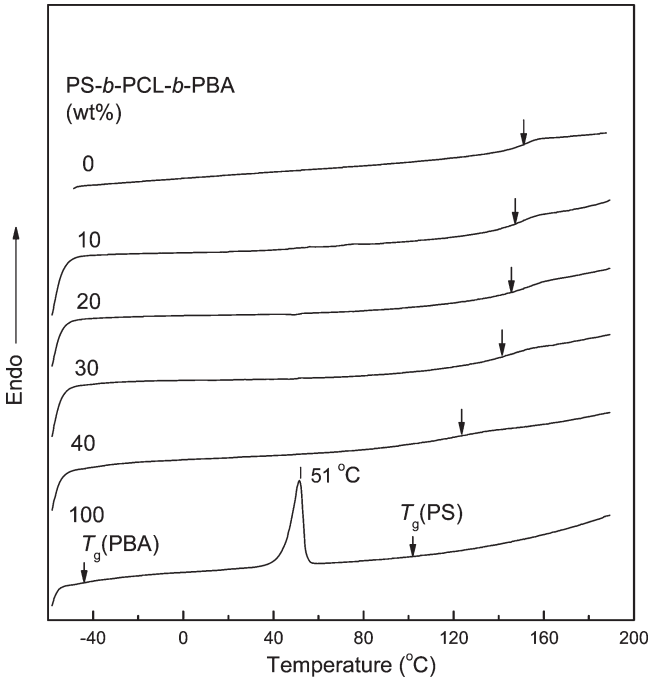

Figure 9. DSC curves of control epoxy, PS-*b*-PCL-*b*-PBA and their nanostructured blends.

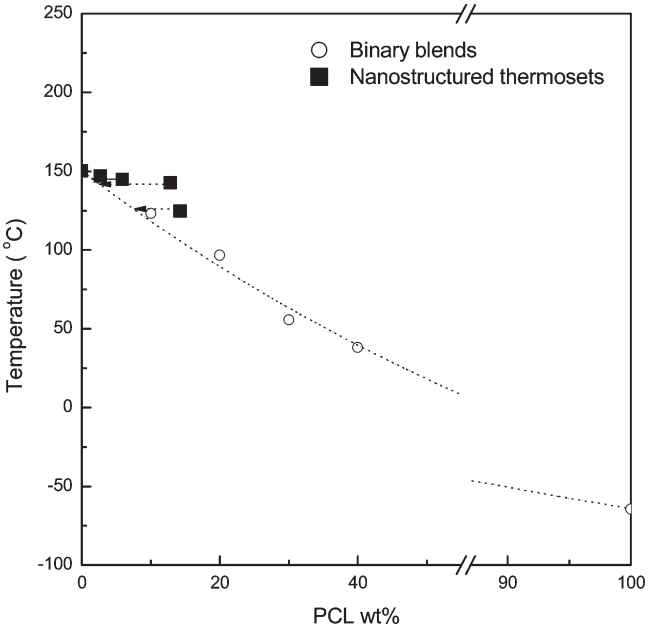

Figure 10. Plots of glass transition temperature of the binary thermosetting blends of epoxy with the model PCL (M_n = 8800) as functions of PCL contents.

and empirical equations.[60−62] Of them, the Couchman equation[62] is frequently used:

$$\ln T_g = [W_1 k \ln T_{g1} + W_2 \ln T_{g2}]/(W_1 k + W_2) \quad (2)$$

where W_i is the weight fraction of component i and T_g is the glass transition temperature of blend; the parameter k is Couchman coefficient defined by:

$$k = \Delta C_{p1}/\Delta C_{p2} \quad (3)$$

where ΔC_{pi} designates the increment of the heat capacity of the specimen at glass transition. In the present case, the value of k was determined to be 1.13 while the binary blends of epoxy thermoset with the PCL having the identical molecular weight with the length of PCL block in the block copolymers were investigated as shown in Figure 10 (the DSC curves not shown here for brevity). Under the identical condition, the nanostructured epoxy thermosets containing PS-*b*-PCL-*b*-PBA triblock copolymers were measured and the plots of T_g's as functions of the concentration of PCL for the nanostructured thermosets are also incorporated in Figure 10. It is seen that the experimental T_g values of the nanostructured thermosets were above the curve of T_g versus the content of PCL for the binary blends of epoxy with the model PCL. This observation indicates that with the identical content of PCL the nanostructured thermosets displayed higher T_g of epoxy matrix than the binary blends. The increased T_g's could be associated with the formation of the nanostructures in the thermosets containing PS-*b*-PCL-*b*-PBA. In the binary blends, the model PCL chains were homogeneously dispersed into the epoxy matrix and were well interpenetrated into the cross-linked epoxy networks via the formation of the intermolecular hydrogen bonding interactions.[54,55] In contrast, the PCL chains have to be enriched at the surfaces of the PS and PBA nanodomains in the nanostructured thermosets due to the connectivity of the polymer blocks. Because of the steric hindrance, the PCL chains at the intimate surface of PS and PBA nanodomains could not be well mixed with epoxy matrix and thus the plasticization of PCL chains on the epoxy matrix would be effectively weakened, which causes the increased T_g's of epoxy matrix. The quantity of demixed PCL can be estimated according to the T_g-composition curve of the binary blends of epoxy with the model PCL and the experimental T_g's of the nanostructured thermosets. The fractions of the demixed PCL subchains were *c.a.* 66, 74, 79, and 46 wt % for the nanostructured thermosets containing 10, 20, 30, and 40 wt % PS-*b*-PCL-*b*-PBA triblock copolymer, respectively. It is of interest to note that with the occurrence of curing reaction the majority of PCL block was demixed from the epoxy matrix but the nanostructures were still preserved. It should be pointed out that the calculation of the quantity of the demixed PCL chains for the nanostructured thermosets on the basis of the T_g-composition relation could be subject to some overestimation because of the following factors: (i) the effect of free volume. The PCL blocks in the nanostructured thermosets were bound to PBA and PS blocks whereas the model PCL in its binary blends with epoxy possess two free ends. Therefore, the nanostructured thermosets displayed the higher T_g's than the model blends owing to the lower free volume in the thermosets; (ii) the difference in PCL conformation. In the nanostructured thermosets the PCL blocks must be extended between the adjacent microdomains of PS and PBA whereas there is no such a restriction in the binary blends of epoxy with the model PCL.

Conclusions

The PS-*b*-PCL-*b*-PBA ABC triblock copolymer was synthesized through the combination of atom transfer radical polymerization (ATRP), copper-catalyzed Huisgen 1,3-dipolar cycloaddition and ring-opening polymerization (ROP). The ABC triblock copolymer was incorporated into epoxy resin and the nanostructured thermosets were obtained. Depending on the concentration of the triblock copolymer several type of nanophases were formed in the thermosets. At the higher content of the triblcok copolymer, these nanophases were arranged in lamellar lattice. It is judged that the formation of the nanostructures in the thermosetting blends follow a double reaction-induced microphase separation mechanism involving PBA and PS blocks.

The studies on the model thermosetting systems showed that the reaction-induced phase separation of the model PBA in epoxy occurred at the conversions much lower than that of the model PS. It is proposed that the PBA nanophases were formed prior to the PS nanophase in the thermosetting blends and the microdomains of PBA subchains could behave as the template for the demixing of PS blocks. Thermal analysis shows that the formation of the nanostructures in the thermosets caused that a part of poly(ε-caprolactone) subchains were demixed from epoxy matrix with the occurrence of curing reaction; the fractions of demixed PCL blocks were estimated according to the T_g-composition relation of the model binary blends of epoxy and PCL.

Acknowledgment. Financial support from Natural Science Foundation of China (No. 20474038 and 50873059) and National Basic Research Program of China (No. 2009CB930400) is gratefully acknowledged. The authors thank the Shanghai Synchrotron Radiation Facility under the projects of No. 10sr0260 & 10sr0126 and Shanghai Leading Academic Discipline Project (Project Number: B202) for partial support.

References and Notes

(1) Williams., R. J. J.; Rozenberg, B. A.; Pascault, J. P. *Adv. Polym. Sci.* **1997**, *128*, 95.
(2) Pascault, J. P.; Williams, R. J. J. In *Polymer Blends*; Paul, D. R., Bucknall, C. B., Eds.; Wiley: New York, 2000; Vol. *1*, pp 379−415.
(3) Chen, J. L.; Chang, F.-C. *Macromolecules* **1999**, *32*, 5348.
(4) Remiro, P. M.; Cortazar, M. M.; Calahorra, M. E.; Calafel, M. M. *Macromol. Chem. Phys.* **2001**, *202*, 1077.
(5) Guo, Q.; Harrats, C.; Groeninckx, G.; Reynaers, H.; Koch, M. H. J. *Polymer* **2001**, *42*, 6031.
(6) Zheng, S.; Zheng, H.; Guo, Q. *J. Polym. Sci., Part B: Polym. Phys.* **2003**, *41*, 1085.
(7) Huang, H. L.; Goh, S. H.; Wee, A.T. S. *Polymer* **2002**, *43*, 2861.
(8) Luo, X.; Zheng, S.; Zhang, N.; Ma, D. *Polymer* **1994**, *35*, 2619.
(9) Zheng, S.; Zhang, N.; Luo, X.; Ma, D. *Polymer* **1995**, *36*, 3609.
(10) Woo, E. M.; Bravenec, L. D.; Seferis, J. C. *Polym. Eng. Sci.* **1994**, *34*, 1664.
(11) Girard-Reydet, E.; Sautereau, H.; Pascault, J. P. *Polymer* **1999**, *40*, 1677.
(12) Jansen, B. J. P.; Meijer, H. E. H.; Lemstra, P. J. *Polymer* **1999**, *40*, 2917.
(13) Galante, M. J.; Borrajo, J.; Williams, R. J. J.; Girard-Reydet, E.; Pascault, J. P. *Macromolecules* **2001**, *34*, 2686.
(14) Zheng, S. In *Epoxy Polymers: New Materials and Innovations*; Pascault, J. P., Williams, R. J. J., Eds.; Wiley-VCH: Weinheim, Germany, 2010; pp 79−108.
(15) Meng, F.; Zheng, S.; Zhang, W.; Li, H.; Liang, Q. *Macromolecules* **2006**, *39*, 711.
(16) Meng, F.; Zheng, S.; Li, H.; Liang, Q.; Liu, T. *Macromolecules* **2006**, *39*, 5072.
(17) Serrano, E.; Tercjak, A.; Kortaberria, G.; Pomposo, J. A.; Mecerreyes, D.; Zafeiropoulos, N. E.; Stamm, M.; Mondragon, I. *Macromolecules* **2006**, *39*, 2254.
(18) Meng, F.; Zheng, S.; Liu, T. *Polymer* **2006**, *47*, 7590.
(19) Sinturel, C.; Vayer, M.; Erre, R.; Amenitsch, H. *Macromolecules* **2007**, *40*, 2532.
(20) Xu, Z.; Zheng, S. *Macromolecules* **2007**, *40*, 2548.
(21) Meng, F.; Xu, Z.; Zheng, S. *Macromolecules* **2008**, *41*, 1411.
(22) Fan, W.; Zheng, S. *Polymer* **2008**, *49*, 3157.
(23) Fan, W.; Wang, L.; Zheng, S. *Macromolecules* **2009**, *42*, 327.
(24) Ocando, C.; Tercjak, A.; Martín, M. D.; Ramos, J. A.; Campo, M.; Mondragon, I. *Macromolecules* **2009**, *42*, 6215.
(25) Amendt, M. A.; Chen, L.; Hillmyer, M. A. *Macromolecules* **2010**, *43*, 3924.
(26) Hillmyer, M. A.; Lipic, P. M.; Hajduk, D. A.; Almdal, K.; Bates, F. S. *J. Am. Chem. Soc.* **1997**, *119*, 2749.
(27) Lipic, P. M.; Bates, F. S.; Hillmyer, M. A. *J. Am. Chem. Soc.* **1998**, *120*, 8963.
(28) Mijovic, J.; Shen, M.; Sy, J. W.; Mondragon, I. *Macromolecules* **2000**, *33*, 5235.
(29) Grubbs, R. B.; Dean, J. M.; Broz, M. E.; Bates, F. S. *Macromolecules* **2000**, *33*, 9522.
(30) Dean, J. M.; Lipic, P. M.; Grubbs, R. B.; Cook, R. F.; Bates, F. F. *J. Polym. Sci., Part B: Polym. Phys.* **2001**, *39*, 2996.
(31) Guo, Q.; Thomann, R.; Gronski, W. *Macromolecules* **2002**, *35*, 3133.
(32) Ritzenthaler, S.; Court, F.; Girard-Reydet, E.; Leibler, L.; Pascault, J. P. *Macromolecules* **2002**, *35*, 6245.
(33) Dean, J. M.; Verghese, N. E.; Pham, H. Q.; Bates, F. S. *Macromolecules* **2003**, *36*, 9267.
(34) Ritzenthaler, S.; Court, F.; Girard-Reydet, E.; Leibler, L.; Pascault, J. P. *Macromolecules* **2003**, *36*, 118.
(35) Rebizant, V.; Abetz, V.; Tournihac, T.; Court, F.; Leibler, L. *Macromolecules* **2003**, *36*, 9889.
(36) Rebizant, V.; Venet, A. S.; Tournillhac, F.; Girard-Reydet, E.; Navarro, C.; Pascault, J. P.; Leibler, L. *Macromolecules* **2004**, *37*, 8017.
(37) Dean, J. M.; Grubbs, R. B.; Saad, W.; Cook, R. F.; Bates, F. S. *J. Polym. Sci., Part B: Polym. Phys.* **2003**, *41*, 2444.
(38) Wu, J.; Thio, Y. S.; Bates, F. S. *J. Polym. Sci., Part B: Polym. Phys.* **2005**, *43*, 1950.
(39) Zucchi, I. A.; Galante, M. J.; Williams, R. J. J. *Polymer* **2005**, *46*, 2603.
(40) Thio, Y. S.; Wu, J.; Bates, F. S. *Macromolecules* **2006**, *39*, 7187.
(41) Ocando, C.; Serrano, E.; Tercjak, A.; Peña, C.; Kortaberría, G.; Calberg, C.; Grignard, B.; Jerome, R.; Carrasco, P. M.; Mecerreyes, D.; Mondragon, I. *Macromolecules* **2007**, *40*, 4086.
(42) Maiez-Tribut, S.; Pascault, J. P.; Soulé, E. R.; Borrajo, J.; Williams, R. J. J. *Macromolecules* **2007**, *40*, 1268.
(43) Yi, F.; Zheng, S.; Liu, T. *J. Phys. Chem. B* **2009**, *113*, 11831.
(44) Hu, D.; Xu, Z.; Zeng, K.; Zheng, S. *Macromolecules* **2010**, *43*, 2960.
(45) Fan, W.; Wang, L.; Zheng, S. *Macromolecules* **2009**, *42*, 327.
(46) Wang, J. S.; Matyjaszewski, K. *J. Am. Chem. Soc.* **1995**, *117*, 5614.
(47) Liu, Q.; Chen, Y. *J. Polym. Sci., Part A: Polym. Chems.* **2006**, *44*, 6103.
(48) Tanaka, H.; Nishi, T. *Phys. Rev. A* **1989**, *39*, 783.
(49) Rasband, W. S. *ImageJ* by U.S. National Institutes of Health, Bethesda, MD, 2007. Please see http://rsb.info.nih.gov/ij/index.html, accessed July 2009
(50) Rostovtsev, V. V.; Green, L. G.; Fokin, V. V.; Sharpless, K. B. *Angew. Chem., Int. Ed.* **2002**, *41*, 2596.
(51) Binder, W. H.; Sachsenhofer, R. *Macromol. Rapid Commun.* **2007**, *28*, 15.
(52) Nandivada, H.; Jiang, X.; Lahann, J. *Adv. Mater.* **2007**, *19*, 2197.
(53) Lutz, J. F. *Angew. Chem., Int. Ed.* **2007**, *46*, 1018.
(54) Yin, M.; Zheng, S. *Macromol. Chem. Phys.* **2005**, *206*, 929.
(55) Ni, Y.; Zheng, S. *Polymer* **2005**, *46*, 5828.
(56) Sanja, Z. N.; Kupehela, L. *Polym. Eng. Sci.* **1976**, *28*, 1149.
(57) Ochi, M.; Okasaki, M.; Shimbo, M. *J. Polym. Sci., Part B: Polym. Phys.* **1982**, *20*, 89.
(58) Shibanov, Y. D.; Godovsky, Y. K. *Prog. Colloid Polym. Sci.* **1989**, *80*, 110.
(59) van Krevelen, D. W. *Properties of Polymers: Their Correlation with Chemical Structures; Their Numerical Estimation and Prediction from Additive Group Contributions*, 4th ed.; Elsevier: Amsterdam, 2009; p 215.
(60) Fox, T. G. *Bull. Am. Phys. Soc.* **1956**, *1*, 123.
(61) Gordon, M.; Taylor, J. S. *J. Appl. Chem.* **1952**, *2*, 496.
(62) Couchman, P. R. *Macromolecules* **1978**, *11*, 1156.